

IMPROVED SHORT COIL CORRECTION FACTOR FOR INDUCTION HEATING OF BILLETS

Mark William Kennedy¹, Shahid Akhtar¹, Jon Arne Bakken¹, Ragnhild E. Aune^{1,2}

¹Department of Material Science and Engineering, Norwegian University of Science and Technology, N-7491 Trondheim,
NORWAY

²Department of Materials Science and Engineering, Royal Institute of Technology, 100 44
Stockholm,
SWEDEN

Communicating author: ragnhild.aune@ntnu.no

Keywords: Induction, heating, billet, short coil, magnetic field

Abstract

To determine the heating rate of billets using ‘short coils’, an appropriate correction factor must be applied to the theoretical relationship. In 1945, Vaughan and Williamson published a semi-empirically modified Nagaoka coefficient applicable for moderate frequency induction heating processes (10 kHz). Recently it was demonstrated that the method of Vaughan and Williamson gives <10% error in the estimated power when heating aluminum billets at 50 Hz.

In the present study, experiments have been conducted on aluminum billets in order to verify an empirical frequency corrected ‘short coil’ equation. Measurements of electrical conductivity ($\pm 0.5\%$), current ($\pm 1\%$), heat ($\pm 1-3\%$), and magnetic flux density ($\pm 1-2\%$) have been performed. The results are compared with 1D analytical calculations, and 2D axial symmetric FEM modeling using COMSOL 4.2[®]. The frequency corrected equation has proven to provide accurate predictions of power (<4% error) within the frequency range 50 Hz to 500 kHz.

Introduction

Induction heating is commonly applied to the re-heating of billets before forging or extrusion processes. The resistive heating produced by eddy currents in the solid or semi-solid work piece during this procedure, is driven by the time varying magnetic flux density in the air-gap between the work piece and the coil. The flux in the air-gap is created by the current flowing in the induction coil, i.e. the magneto-motive force. In Figure 1 it can be seen that the currents present in the work piece are concentrated in the outer ‘shell’, or the first electromagnetic penetration depth (δ_w), and flow in a direction which opposes the magnetic field produced by the induction coil.

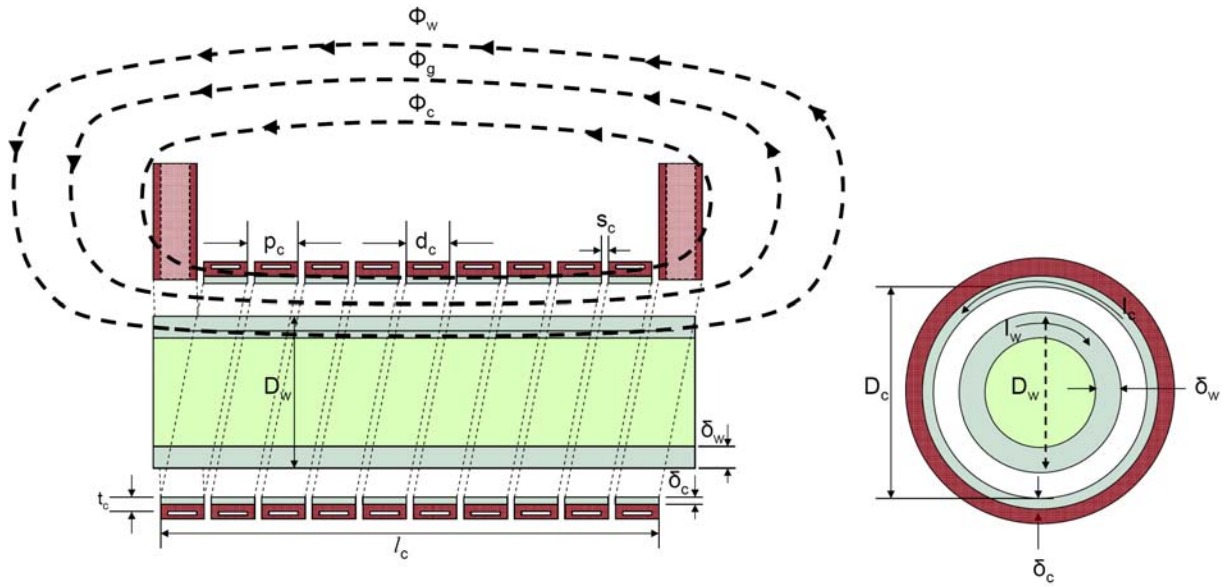


Figure 1. Schematic drawing of a 10 turn induction coil with a billet slightly longer than the coil [1]. (D_c = inner diameter of the coil [m]; D_w = outer diameter of the work piece [m]; l_c = length of the coil [m]; l_w = length of the work piece [m]; I_c = current in the coil [A, RMS]; I_w = current in the work piece [A, RMS]; δ_c = electromagnetic penetration depth in the coil [m]; δ_w = electromagnetic penetration depth in the work piece [m]; t_c = conducting thickness of the coil [m]; p_c = pitch of the coil [m]; d_c = width of the coil [m]; s_c = spacing of the coil [m]; Φ_c , Φ_g and Φ_w are the coil magnetic fluxes linking the coil, air gap and work piece respectively [Wb].)

Flux Densities of Long and Short Air-Core Coils

The magnetic flux density of a very ‘long coil’ can be predicted using the infinite coil formula:

$$|\vec{B}_\infty| = \frac{\mu_o \mu_r N_c I_c}{l_c} \quad (1)$$

where B_∞ is the axial flux density of an infinite coil [T], μ_o the magnetic permeability of the free space ($4\pi \times 10^{-7}$ [H/m]), μ_r the relative magnetic permeability, N_c the number of coil turns, I_c the coil RMS current [A], and l_c the length of the coil [m]. However, coils used for induction heating are typically short and Equation (1) can not accurately estimate their magnetic flux density. When Equation (1) is multiplied by a ‘short coil’ correction factor, a more accurate estimate of the average z-component of the magnetic flux density is obtained for a typical induction coil.

It is important to point out that ‘short coil’ correction factors, such as the Nagaoka coefficient [2], have been found from the analytical solution of the inductance of a ‘short coil’, starting with a current sheet approximation. However, the Nagaoka coefficient can be estimated using numerical solvers to high accuracy, interpolated from the original 6 digit tabulated values, or estimated to approximately 3 significant digits, using the following relationships [3]:

$$k_N = \frac{1}{1 + 0.4502 \left(\frac{D_c + \delta_c}{l_c} \right)} \quad (2)$$

$$\delta_c = \left(\frac{\rho_c}{\pi \mu_o \mu_r f} \right)^{0.5} \quad (3)$$

where k_N is the Nagaoka ‘short coil’ correction factor, D_c the diameter of the coil [m], δ_c the electromagnetic penetration depth into the coil [m], ρ_c the electrical resistivity of the coil [Ωm], and f the frequency [Hz].

Flux Densities of Short Coils Containing a Work Piece

If a high electrical conductivity work piece is inserted into an induction coil, the penetration of the magnetic flux from the air-gap into the work piece is greatly reduced. The flux in the air-gap is thereby increased significantly and becomes more uniform in both the axial and radial directions, as indicated in Figure 2 for a work piece of electrical grade aluminum billet.

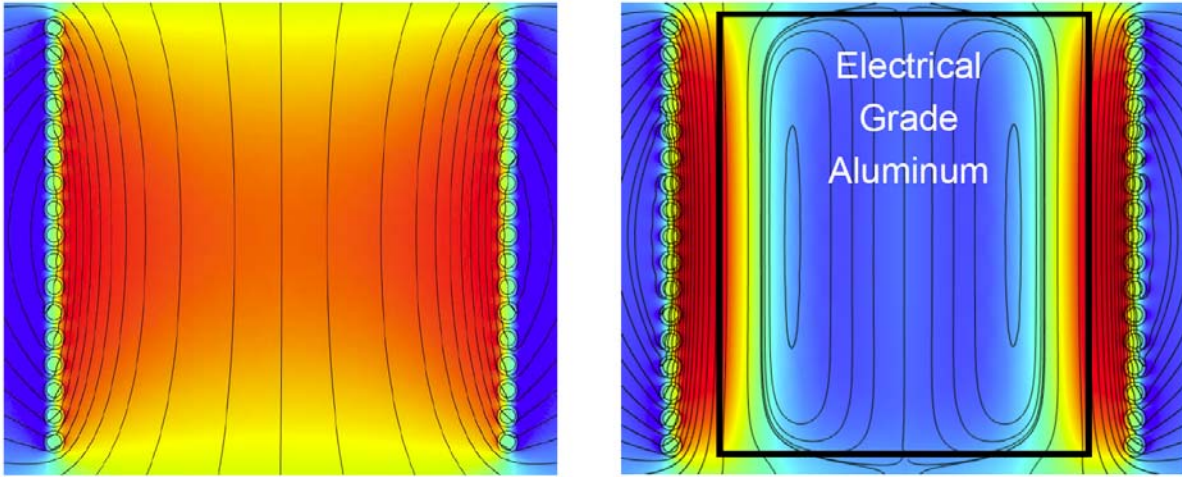


Figure 2. COMSOL 4.2[®] simulation showing the impact of the work piece on the magnetic flux density in the air-gap of a ‘short coil’ (17 turn), $D_c/l_c=1.0$, 50 Hz.

As early as 1945, Vaughan and Williamson [4] proposed an empirical modification of the Nagaoka ‘short coil’ correction factor, based on the fraction of the volume of the air-gap occupied by the work piece. Experiments were conducted by Vaughan and Williamson at 10 kHz using non-magnetic cylindrical work pieces of brass, copper and 18-8 stainless steel to verify the general validity of their equation as given by the following relationship:

$$k_N^* = k_N \left(1 - \left(\frac{D_w}{D_c} \right)^2 \right) + \left(\frac{D_w}{D_c} \right)^2 \quad (4)$$

where k_N^* is the modified Nagaoka ‘short coil’ correction factor, and D_w the diameter of the work piece [m].

The present authors have recently proposed a modification to Equation (4) to account for variations in the electromagnetic penetration into both the coil and the work piece [5], i.e.:

$$k_N^* = k_N \left(1 - \left(\frac{D_w - \delta_w}{D_c + \delta_c} \right)^2 \right) + \left(\frac{D_w - \delta_w}{D_c + \delta_c} \right)^2 \quad (5)$$

$$\delta_w = \left(\frac{\rho_w}{\pi \mu_o \mu_r f} \right)^{0.5} \quad (6)$$

where δ_w is the electromagnetic penetration depth into the work piece, and ρ_w is the electrical resistivity of the work piece [Ωm].

The magnetic flux density present in the air-gap of a ‘short coil’ containing a work piece can then be calculated using Equations (1), (2), (3), (5) and (6). As Equation (5) is a one dimensional correction factor, it represents the integral average flux density over the full length and area of the coil air-gap. For round coils it has, however, been found adequate to equate $(D_c + \delta_c)$ to the average coil diameter, over a wide range of frequencies from 50 Hz to 500 kHz [5].

Induction Heating Using Short Coils

The classical approach for the computation of heat generation in cylindrical work pieces [1] has been reviewed prior to the present study, and the required equations can be summarized as follows:

$$P_w = k_N^{*2} \sqrt{2} \pi (I_c N_c)^2 \rho_w \xi_w \varphi(\xi_w) / l_c \quad (7)$$

$$\xi_w = \frac{D_w}{\delta_w \sqrt{2}} \quad (8)$$

$$\varphi(\xi_w) = \frac{\sqrt{2} (ber \xi_w ber' \xi_w + bei \xi_w bei' \xi_w)}{ber^2(\xi_w) + bei^2(\xi_w)} \quad (9)$$

where P_w is the heat generated in the work piece [W], φ a correction factor accounting for the average phase shift between current and voltage in the work piece, and ξ_w a dimensionless penetration or reference depth, that is found in many of the equations in classical induction heating literature. ber , ber' , bei and bei' are the real and imaginary parts of the zero order modified Kelvin Bessel functions and their derivatives, the solutions to which can be found using numerical solvers [6], look-up tables [7] or graphs [1].

Equation (7) can be used with the ‘short coil’ correction factor presented in Equation (5) to find the power induced by the ‘short coil’ in a work piece of length equal to or greater than that of the coil. If the work piece is shorter than the coil, Equation (7) can still be used, substituting the length of the work piece for the length of the coil.

Experimental Conditions and Procedures

In the present study, different sets of experiments have been performed to determine the actual heating rates and magnetic flux densities produced by different work piece and coil geometries, as a means of validating Equation (5). Some of the heating results will be presented in this publication, while more results including the magnetic field measurements will be presented elsewhere [8-9]. A schematic drawing of the main part of the experimental apparatus used is shown as Figure 3.

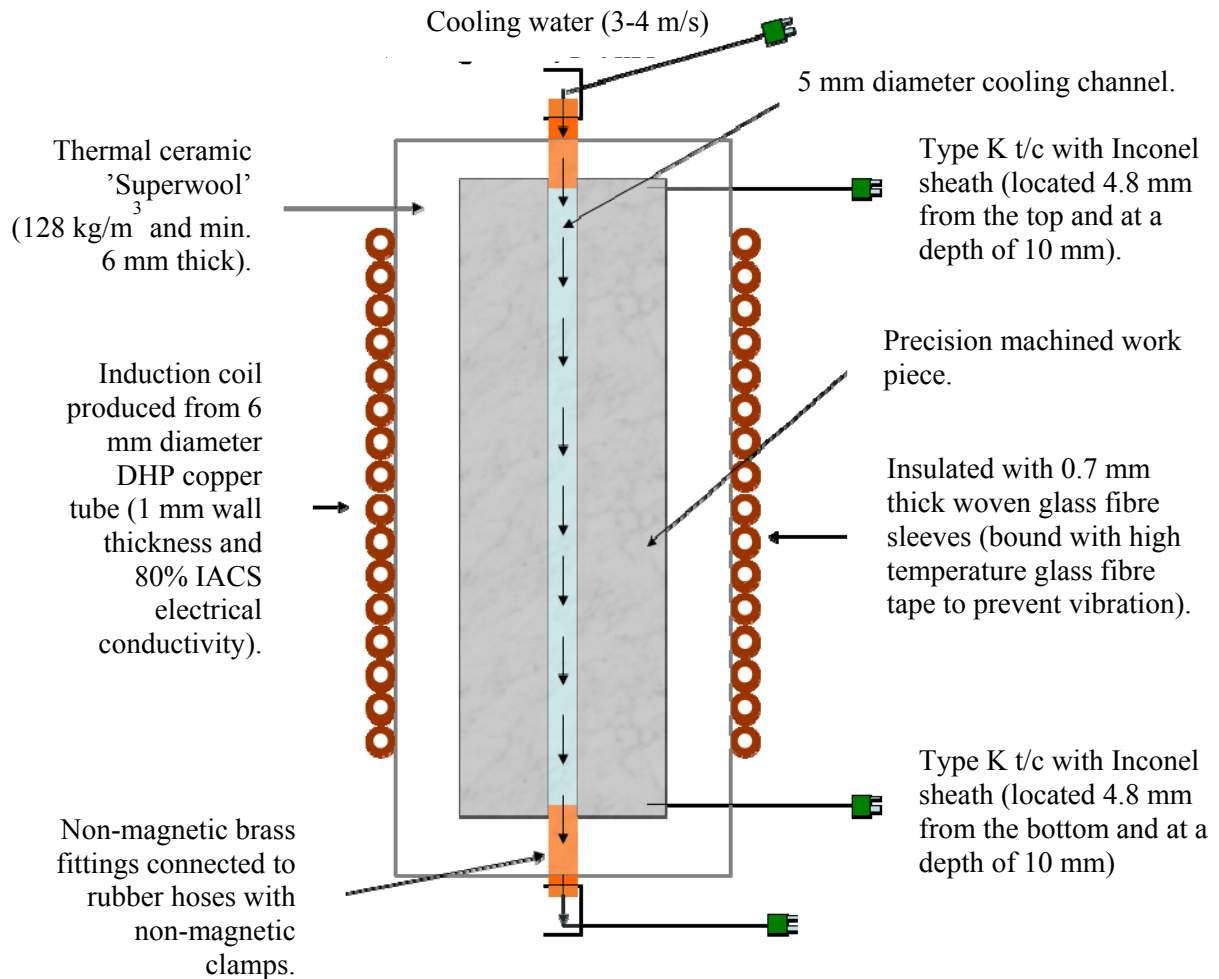


Figure 3. Schematic drawing of the water cooled induction heating experimental apparatus [8].

Thermal or 'calorific' heating measurements were performed, while applying a constant voltage to the coil. During the measurements, the temperatures of the thermocouples were carefully monitored, as well as the current flowing in the coil. When both electrical and thermal stability had been reached, a number of electrical readings were taken over a period of about 5 to 20 minutes, while the flow rate of the cooling water was logged simultaneously with the thermocouple data.

The electrical conductivity of the aluminum work pieces were measured using an AutoSigma 3000 conductivity analyzer (General Electric Inspection Technologies, UK) to an accuracy of

$\pm 0.5\%$. The instrument was calibrated prior to use against aluminum standards accurate to $\pm 0.01\%$ IACS [10]. Measurements were taken on both the machined ends of each work piece. An average of approximately 75 readings was used to estimate the room temperature conductivity of each work piece.

Power measurements were taken using a Fluke 43B power quality analyzer (Fluke, USA), with a resolution of $\pm 100\text{W}$. Coil current measurements were made with an i1000S inductive current probe (Fluke, USA) with an accuracy of $\pm 1\%$ and a resolution of 1A. The electrical data measured in the present study represents an average value based on 2 to 8 readings, while operating at steady state thermal conditions.

The water flow rate was determined using a scale which had a capacity of 100 kg and a resolution of 0.01 kg. The total weight difference over the hundreds of seconds used for each power estimation was then used to calculate the average water flow rate with $< 0.1\%$ error.

Billets of two different alloys, i.e. billets (i) with different IACS electrical conductivities and (ii) with different dimensions, as well as a number of different coil geometries were operated in 10 separate experiments at 50 Hz. The main properties of the work pieces and coils are summarized in Tables I and II.

Table I. The Main Properties of the Work Pieces used in the Billet Heating Experiments [8]

Work Pieces	1	2	3
Alloy	A356	6060	6060
Diameter, mm	75.0	95.0	95.0
Length, mm	130.0	130.0	260.0
Measured IACS Electrical Conductivity, %	48.4	56.2	53.4
Penetration depth δ_w (mm) at 50 Hz and 293 K from Equation (6)	13.43	12.47	12.79
ξ_w from Equation (8)	3.948	5.388	5.252
$\phi(\xi_w)$ from Equation (9)	0.823	0.862	0.859
Coil 1	1-1	1-2	
Coil 2		2-2	
Coil 3			3-3

Table II. The Main Properties of the Coils used in the Billet Heating Experiments [8]

Coils	Short Coil 1	Short Coil 2	Long Coil 3
Average Diameter, mm	132	155	132
Height, mm	106	108	218
Diameter to Height Ratio	1.24	1.44	0.60
Number of Turns	16	16	32
Short Coil Correction Factor from Equation (2)	0.641	0.607	0.786
Electrically Determined IACS Conductivity, %	80	80	80
Penetration depth δ_c (mm) at 50 Hz and 293 K from Equation (3)	10.45	10.45	10.45
Modified Nagaoka Coefficient kN^* for Work Piece 1 from Equation (5)	0.720		
Modified Nagaoka Coefficient kN^* for Work Piece 2 from Equation (5)	0.783	0.718	
Modified Nagaoka Coefficient kN^* for Work Piece 3 from Equation (5)			0.870

Results and Discussion

The validation of the proposed 1D correction factor presented in Equation (5) can best be accomplished by the comparison of the predicted analytical heating rate with the measured heating rate. This represents an ‘integral’ along both the length and phi directions of the work piece. As the heating rate obtained in a particular magnetic field is proportional to the square of the magnetic flux density, errors in Equation (5) are magnified in the error of the measured heating rates. This is indicated in Equation (7), making the suggested approach a particularly sensitive validation method.

The obtained data from the 10 heating experiments are summarized in Table III (5 conditions and 5 duplicates). As can be seen from the table, the average current and work piece electrical conductivity (evaluated at the average aluminum temperature) were used in evaluating Equation (7) and further used as input values in COMSOL 4.2[®] to derive estimates of the heating rate. Both the analytical approach and COMSOL 4.2[®] model excludes heat losses, i.e. the work piece is assumed to be perfectly insulated. The obtained values have also been added into Table III, together with the values calculated for the ‘electrical’ power, obtained as a result of the difference in the coil resistance with and without a work piece and the measured current.

Table III. Summary of the Experimental Data (with Duplicates) Obtained in the Present Study, and other Values of Importance used in the Analysis [8]

Coil (#)	Work Piece (#)	Average Aluminum Electrical Resistivity ($\Omega \text{ m}$) $\times 10^{-8}$ *	Current (A)	Heating Power Calorific (W)	Heating Power Electrical (W)	Electrical Calorific Absolute Difference (%)	Heating Power COMSOL (W)	COMSOL Calorific Absolute Difference (%)	Heating Power Analytical Equation (7) (W)	Analytical Calorific Absolute Difference (%)
1	1	3.76	1001.3	636	631	0.9	623	2.1	659	3.6
1	1	3.76	1001.0	634	611	3.6	623	1.7	659	3.9
1	2	3.44	1028.0	975	N/A	N/A	976	0.1	1035	6.1
1	2	3.42	1025.4	954	1019	6.8	970	1.6	1029	7.9
2	2	3.27	909.5	642	688	7.2	618	3.7	658	2.5
2	2	3.26	908.8	643	703	9.2	617	4.1	657	2.2
3	3	3.58	893.5	1884	2117	12.3	1888	0.2	1910.6	1.4
3	3	3.58	891.8	1894	2132	12.6	1881	0.7	1903.2	0.5
3	3	3.30	557.8	746	732	1.8	713	4.4	721.4	3.2
3	3	3.30	558.0	736	727	1.2	713	3.0	721.8	1.9
		* see [9]			Average:	6.2	Average:	2.2	Average:	3.3

The resulting uncertainty in the thermal heating estimate is believed to be primarily due to the obtained accuracy of $\pm 0.05^\circ\text{C}$ in the thermocouple delta-temperature. This temperature accuracy calculated as a fraction of the actual measured delta-temperature of the billet cooling water, represents an average uncertainty of less than 2%.

The heat losses ($< 0.6\%$, average of 0.4%) were estimated using a typical thermal conductivity value ($k_{insulation}$) for the Thermal Ceramics ‘Superwool’ used in the present experiments ($\sim 0.02 \text{ W/m/K}$) [11], and the actual thickness of the insulation used in each case. The insulation thickness varied depending upon the work piece, as well as the coil geometry.

Both estimates of heating presented in Table III, i.e. the analytical values and the COMSOL 4.2[®] values, have been plotted in Figure 4 along side the experimental data. As can be seen from Figure 4, there is good agreement between all the values. Only the electrical data for Coil #3 and

Work Piece #3 at high current have any significant errors. In these cases, the change in the coil operating temperature and resulting electrical conductivity, between the measurements made with an air-core and with the work piece, has been determined to be the main parameter causing the deviations.

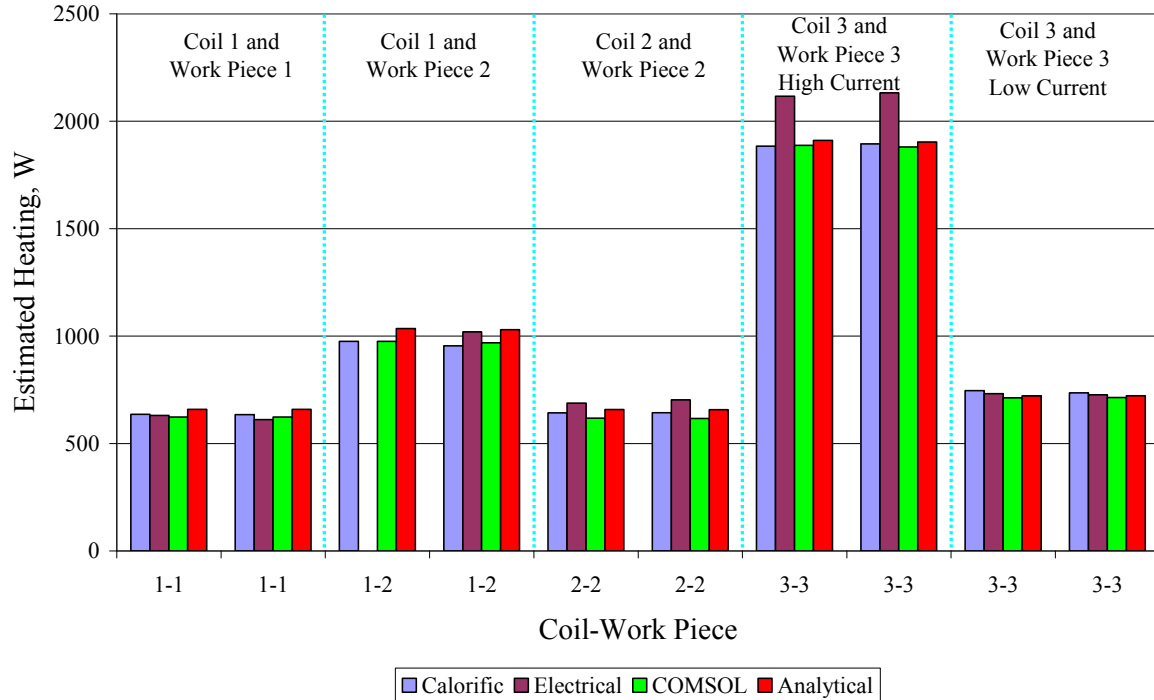


Figure 4. Experimental heating data resulting from calorific and electrical methods are compared with the estimates from the COMSOL 4.2[®] and the analytical modeling approach. Data are in the same order as listed in Table III, with 5 conditions and 5 duplicates [8].

From Table III it can be seen that the relative errors in the analytical heating estimates are lower for the ‘long’ Coil #3. This is believed to be the result of the initial ‘air-core’ Nagaoka coefficient being closer to unity and thus requiring less correction. Due to this, the data for Coil #1 and Work Piece #1, as well as for the larger diameter Coil #2 and Work Piece #2, should theoretically represent the most challenging cases for the proposed equations, i.e. Equations (5) and (7).

It can also be seen from Table III that the average difference in the estimated heat (power) resulting from both the COMSOL 4.2[®] and the analytical approach, is less than that of the electrical data when compared with the calorifically determined heating power. Given that the FEM model, as well as the analytical model is not considering the heat losses, it is believed that the heating estimates should be high by the average heat loss of 0.4%. In other words, the COMSOL 4.2[®] estimate has an error of < 2%, and analytical modeling estimates of < 3% when compared with the experimental calorific data.

Comparison between Analytical Model and COMSOL FEM at Different Frequencies

A virtual experiment has also been performed comparing estimates of heating (power) as a function of frequency using the proposed analytical model against the COMSOL 4.2[®] model. Coil #1 and Work piece #1, which represent a challenging case due to the low length to diameter ratio, as well as the relatively large air-gap (low k_N^*), was used for the comparison. The following conditions were chosen, i.e. current of 1001 A, temperature of 37.1°C and $\rho_w = 3.76E^{-8} \Omega m$.

In Table IV the calculated estimates of heating (power) are presented. As can be seen, an offset of approximately 4% exists between the two models and this deviation appears to be consistent in the frequency range from 50 Hz to 500 kHz. The good agreement between the COMSOL 4.2[®] estimates and the experimental results at 50 Hz, appears to indicate that the obtained deviation in the analytical power estimate from Equation (7) is a result of the empirical nature of Equation (5). This 4% bias is particular to this geometry, a lower bias (0.8%) was found for the longer more ‘ideal’ Coil #3 [9].

Table IV. Comparison between the Estimates of Heating (Power) as a Function of Frequency for Coil #1 and Work piece #1. The Values are Based on the Analytical and COMSOL 4.2[®] Modeling Approaches [8]

Frequency (Hz)	Experimental Power (W)	Analytical Power (W)	COMSOL Power (W)	Analytical-COMSOL Difference (%)
50	634	659	623	5.8
500	N/A	2567	2466	4.1
5000	N/A	8672	8370	3.6
50000	N/A	27957	26816	4.3
500000	N/A	88623	85247	4.0
Average:				4.3

Conclusions

An improved ‘short coil’ correction factor has been developed and experimentally validated for use during induction heating of billets at frequencies from 50 Hz to 500 kHz. By adopting the improved correction factor, the errors obtained in the estimates of heating (power) have been reduced from <10% to <4%. The obtained results compare highly favorably with the factor of 2 error that would result from making a ‘long coil’ assumption, i.e. $k_N^* = 1.0$. The improved ‘short coil’ correction factor can be used to estimate the average flux density of a ‘short coil’ with an error of <2% based on the square root of the error in the heating estimation.

Acknowledgements

The present study was carried out as part of the RIRA (Remelting and Inclusion Refining of Aluminium) project funded by the Norwegian Research Council (NRC) - BIP Project No. 179947/I40. The industrial partners involved in the project are: Hydro Aluminium AS, SAPA Heat Transfer AB, Alcoa Norway ANS, Norwegian University of Science and Technology

(NTNU) and SINTEF Materials and Chemistry. The funding granted by the industrial partners and the NRC is gratefully acknowledged.

The authors wish to express their gratitude to Egil Torsetnes at NTNU for helping with the design and construction of the experimental apparatus. Sincere gratitude is also due to Kurt Sandaunet at SINTEF for his support and help, as well as for the use of the SINTEF laboratory.

References

1. M. W. Kennedy, S. Akhtar, J. A. Bakken, and R. E. Aune, "Review of Classical Design Methods as Applied to Aluminum Billet Heating with Induction Coils," EPD Congress, San Diego, California, February 27 - March 3, (2011), 707-722.
2. H. Nagaoka, "The Inductance Coefficients of Solenoids," *Journal of the College of Science*, 27, (1909), 18-33.
3. D. Knight, http://www.g3ynh.info/zdocs/magnetics/part_1.html, accessed September 22, (2011), [Online].
4. J. Vaughan and J. Williamson, "Design of Induction-Heating Coils for Cylindrical Nonmagnetic Loads," *Transactions of the American Institute of Electrical Engineers*, 64, (1945), 587-592.
5. M. W. Kennedy, S. Akhtar, J. A. Bakken, and R. E. Aune, "Analytical and Experimental Validation of Electromagnetic Simulations Using COMSOL[®], re Inductance, Induction Heating and Magnetic Fields," submitted to the COMSOL Users Conference, Stuttgart Germany, October 26-28, (2011).
6. R. Weaver, <http://electronbunker.sasktelwebsite.net/DL/NumericalExamples01.ods>, accessed September 22, (2011), [Online].
7. N. McLachlan, *Bessel Functions for Engineers*, (Gloucestershire, Clarendon Press, 1955), 215 - 230.
8. M. Kennedy, S. Akhtar, J. A. Bakken, and R. E. Aune, "Theoretical and Experimental Validation of Magnetic Fields in Induction Heating Coils," submitted to *IEEE Transactions on Magnetics*, (2011).
9. M. W. Kennedy, S. Akhtar, J. A. Bakken, and R. E. Aune, "Analytical and FEM Modeling of Aluminum Billet Induction Heating with Experimental Verification," submitted to the TMS Light Metals, Orlando Florida, March 11-15, (2012).
10. *Copper Wire Tables Circular No. 31*: US Bureau of Standards, (1913).
11. "Superwool[®] Plus Blanket Datasheet Code EU: 11-5-01 US: 11-14-401," www.thermalceramics.com, accessed August 8, (2011), [Online].